energies

MDPI

Article

Continuous Phenol Removal Using a Liquid–Solid Circulating Fluidized Bed

Nandhini Sureshkumar [1], Samiha Bhat [1], Shwetha Srinivasan [1], Nirmala Gnanasundaram [1,*], Murugesan Thanapalan [2], Rambabu Krishnamoorthy [3], Hatem Abuhimd [4], Faheem Ahmed [5] and Pau Loke Show [6]

1 Mass Transfer Lab, School of Chemical Engineering, Vellore Institute of Technology, Vellore 632014, India; nandhini120698@gmail.com (N.S.); samihabhat17@gmail.com (S.B.); srinivasanshwetha.2009@gmail.com (S.S.)
2 Department of Chemical Engineering, Universiti Tecknologi Petronas, Perak 32610, Malaysia; murugesan@utp.edu.my
3 Department of Chemical Engineering, Khalifa University, Abu Dhabi 127788, UAE; rambabu.krishnamoorthy@ku.ac.ae
4 National Center for Nanotechnology and Semiconductor, King Abdulaziz City for Science and Technology, Riyadh 11564, Saudi Arabia; habuhimd@kacst.edu.sa
5 Department of Physics, College of Science, King Faisal University, P.O. Box-400, Al-Ahsa 31982, Saudi Arabia; fahmed@kfu.edu.sa
6 Department of Chemical and Environmental Engineering, Faculty of Science and Engineering, University of Nottingham Malaysia, Selangor 43500, Malaysia; PauLoke.Show@nottingham.edu.my
* Correspondence: gsnirmala@vit.ac.in

Received: 16 June 2020; Accepted: 24 July 2020; Published: 27 July 2020

Abstract: A liquid-solid circulating fluidized bed (LSCFB) helps to overcome the shortcomings of conventional fluidized beds by using a particle separation and return system as an integral part of the overall reactor configuration. Batch adsorption experiments were carried out for the removal of phenol from a synthetically prepared solution using fresh activated-carbon-coated glass beads. The morphological features and surface chemistry of the adsorbent were analyzed via SEM and FTIR techniques. The adsorbent dosage, contact time and temperature were varied along with solution pH to assess their effects on the adsorbent performance for phenol removal. Isotherm modeling showed that the phenol removal using the activated-carbon glass beads followed the Langmuir model. Effectively, it was observed at an adsorbent loading of 2.5 g/150 mL of feed volume and a contact time of 3 h produced an 80% efficiency in the batch study. Furthermore, on scaling it up to the column, the desired 98% phenol-removal efficiency was obtained with an adsorbent dosage of 250 g and contact time of 25 min. Adsorbent regeneration using 5% (*v*/*v*) ethanol showed a 64% desorption of phenol from the sorbent within 20 min in the LSCFB.

Keywords: circulating fluidized bed; adsorption; activated carbon; phenol; glass beads

1. Introduction

Chemical process industries generate tremendous quantities of wastewater that significantly contribute to aquatic environmental pollution. This has demanded the development of sustainable and effective treatment methodologies for industrial effluents [1]. Design and development of innovative process technology to efficiently handle large volumes of polluted water streams in a relatively shorter time are highly desirable and promising for industrial applications. Phenol is the most commonly present contaminant in the industrial effluent stream. It is known to be highly toxic and causes harmful chronic effects on humans and animals alike [2]. This raises concern over the traces of

phenolic content present in drinking water and the negative externalities caused by their discharge from the effluent treatment plants on the environment [3]. Many technologies have been developed for the decontamination of phenol-polluted wastewater streams, including membrane separation, advanced oxidation, activated sludge, ion exchange and adsorption [4–6]. Out of the various specified technologies, adsorption proves to be the most viable option due to its economic feasibility, ease of scalability and strategic removal of the target compound(s) [7,8]. It offers a wide variety of highly selective adsorbents with a good regeneration potential [9,10]. Since it does not yield any formation of sludge [11], adsorption does not pose any threat to the environment and achieves a high product quality [12,13]. Batch-mode and column-mode are the two major categories of the adsorption operation.

Column adsorption types consist of four main types: a fixed-bed type; continuous moving-bed type; fluidized-bed type and pulsed-bed type. Of these, the fluidized-bed type is widely adopted in industries due to its ability to handle large feed volumes and its easier process control [9]. The fluidized-bed technology offers the salient advantages of improved heat/mass transfer rates, enhanced interfacial contact area and isothermal operation [10]. Within the fluidized-bed column adsorption, the circulating fluidized-bed (CFB) offers effective liquid-solid contact, uniform temperature, high throughputs and better solid holdup control as compared to the conventional fluidized-bed type [11]. Although gas-solid-type CFBs have been vastly investigated from the 1960s, research studies on a liquid-solid CFB (LSCFB) are very scant. The concept of a LSCFB gained momentum around the 1990s and has been explored widely in the last ten years [10]. The LSCFB technique is very promising for various industries, such as pharmaceuticals, biotechnology catalytic refining, wastewater treatment, etc. [9]. In this work, we primarily focused on phenol adsorption studies via a liquid-solid circulating fluidized bed (LSCFB). The usage of LSCFB for phenol adsorption provides significant advantages over the conventional fluidized beds. These advantages include an enhanced adsorption efficiency, high operational simplicity, better yields, high liquid residence times, low chemical consumption, applicability to non-clarified streams and an increase in the interfacial area between the solid and liquid phases [9,12].

With the use of the appropriate solid particles, the LSCFB system would help overcome the limitations of a conventional fluidized bed. To aid the process of fluidization in the column, the adsorbent used in this study is glass beads [13] coated with commercial activated carbon, primarily because of its high density. Epoxy resin was used for coating these beads with activated carbon due to its strong adhesive properties. Before the column studies, batch investigations were conducted to identify the optimized operating conditions for the LSCFB.

2. Materials and Methods

2.1. Materials

Bituminous coal-based commercial activated carbon (Chemviron CPG-LF) was procured from Calgon Carbon, Brazil, for the preparation of the adsorbent beads. The activated carbon has a surface that is non-polar, which results in an affinity for non-polar adsorbates such as organics. The adsorbent particle sizes were in the range of 1.2–1.4 mm with an iodine number of 950 mg/g. The carbon possessed a specific surface area of 650 m^2/g (based on the Brunauer–Emmett–Teller method) with a mean pore radius of 450 nm and total pore volume of 0.18 cm^3/g. Epoxy resin (Araldite 506), methyl nadic anhydride (MNA hardener) and phenol were obtained from Sigma Aldrich, India. Ethanol (99% pure) was obtained from Fisher scientific, India. Glass beads (1.76 mm diameter) were provided in gift packs from local industry in Vellore SIPCOT, India. All the chemicals and reagents used in the study were of analytic grade and were used directly for experiments. Double-distilled water (Merck Millipore) was utilized for the solution preparation, dilution and wash applications.

2.2. Adsorbent Preparation and Characterizations

Activated carbon was used to coat the glass beads with a dimension 1.76 mm in diameter. This coating was achieved by using epoxy resin. The resin and MNA hardener were mixed in the weight ratio of 1:1. The slurry of the glass beads and epoxy resin was made and mixed, such that the resin was distributed evenly on the glass bead surface to ensure uniform binding of the activated carbon. Following this, a known measure of activated carbon was sprinkled into the slurry, and then rolled and sieved to give the resultant activated-carbon glass bead adsorbent.

The morphology and surface chemistry of the synthesized adsorbent beads were analyzed through scanning electron microscopy (SEM) and Fourier transform infrared spectroscopy (FTIR) studies. SEM micrographs (Evo-18, Carl Zeiss, Dublin, CA, USA) were used to understand the pore structure of the activated carbon glass bead samples. An IR spectrophotometer (IR Affinity-1, Shimazdu, Kyoto, Japan) was used to conduct the FTIR analysis of the adsorbent through the KBr pellet method. The spectral scan was acquired in the range from 4000 to 400 cm^{-1}. SEM and FTIR studies were performed for the fresh, phenol-loaded and regenerated activated-carbon glass bead samples.

2.3. Batch Adsorption Studies

The stock solution prepared was a system of phenol and water. It had an initial concentration of 1000 ppm. The as-prepared phenol water system was stable and non-azeotropic. Batch adsorption studies were conducted for analyzing the effect of four operational parameters, namely adsorbent dosage, contact time, pH and temperature, on the adsorbent performance [14]. Four adsorbent dosage values of 1, 1.5, 2 and 2.5 g were examined using 150 mL of the stock solution. The conical flasks were kept in the orbital shaker at standard conditions of 75 rpm and 30 °C. Samples of 10 mL after a specific time duration was pulled out from the conical flasks to measure their pH and phenol concentration. The solution pH was measured using a digital pH system (HQ411, Hach, Berlin, Germany). The phenol concentration in the test samples were determined using a UV–Vis spectrophotometer (2200, Systronics, Chennai, India) at 270 nm using the calibration graph method. A standard calibration graph was obtained initially using known concentrations of phenol in the water standard samples (x-axis) and the respective absorbance for each of the standard sample (y-axis). The phenol concentration for the test samples were obtained by measuring their absorbance value and using this value to acquire the corresponding concentration from the calibration graph [15].

For each adsorbent dosage, the contact time was varied from 0 to 3 h. Test samples were obtained at 0.25, 0.5, 0.75, 1, 2 and 3 h of contact time. For analyzing the effect of temperature, the given adsorbent dosage was subjected to four different temperatures (20, 30, 40, 50 and 60 °C) for 1 h operational time and subjected to spectrophotometry to calculate the final phenol concentrations. To investigate the regeneration capacity of the adsorbent, 5% (v/v) ethanol was used to desorb phenol from the adsorbent while varying the contact time from 0 to 3 h. Test samples were acquired at 0.25, 0.5, 0.75, 1, 2 and 3 h of the regeneration step. The phenol removal percentage was calculated by Equation (1) [16]:

$$\%R = \frac{C_i - C_e}{C_i} \times 100 \quad (1)$$

where C_i and C_e are the phenol concentrations (ppm) of the initial and equilibrium states of adsorption.

The adsorption capacity of the activated-carbon glass beads after time t of adsorption for the adsorbent (q_t) was calculated using Equation (2) [17]:

$$q_t = \frac{(C_i - C_t) \times V_a}{W_a} \quad (2)$$

where C_t (ppm), V_a (L) and W_a (g) are the phenol concentrations after time t, the volume of feed solution taken and the weight of the adsorbent used, respectively. The equilibrium adsorption capacity (q_e) for the adsorbent was calculated from Equation (2) using C_e instead of C_t.

2.4. LSCFB Study

The LSCFB system consisted of three main components—A riser, downcomer and liquid-solid separator, as shown in Figure 1. The proportionate design of the LSCFB system was based on our previous reported work [18]. The riser was of dimensions 1.5 m height and 4 cm diameter. The downcomer measured a height of 1.8 m and a width of 8 cm in diameter. The riser was fitted with two inlet feed lines—A primary feed line and a secondary feed line. The primary feed line was regulated using a rotameter with a flow rate of 3000 L/h and another flow meter of 2400 L/h regulated the secondary pipe inlet. The capacity of the inlet feed tank to the riser for adsorption was 100 L. The riser was provided with two distributors—A primary distributor and a secondary distributor at its bottom. The primary distributor occupied 20% of the total bed area while the secondary distributor was 5% open of the total bed area. The riser had two pressure tapings, one near the lower end of the column above the distributors and the other one at the upper end just before the elbow bend into the liquid-solid separator. These two pressure tapings were connected to a manometer filled by the manometric fluid to record the pressure drop in the column. The top end of the riser was connected to the liquid-solid separator just after the elbow bend. The liquid that overflowed was circulated back to the feed tank while the rest of the contents paved their way to the downcomer through the top dynamic seal. The capacity of the inlet feed tank to the downcomer for desorption was 100 L. A rotameter of 2400 L/h was used to regulate the inlet feed line to the downcomer. The downcomer had a diffuser that uniformly provides an inlet for the desorption liquid. There was a valve provided at the bottom dynamic seal to regulate the solid holdup between the riser and the downcomer. There were provisions for wash water provided at the bottom of the liquid-solid separator and the downcomer. This was operated after every adsorption and desorption cycle.

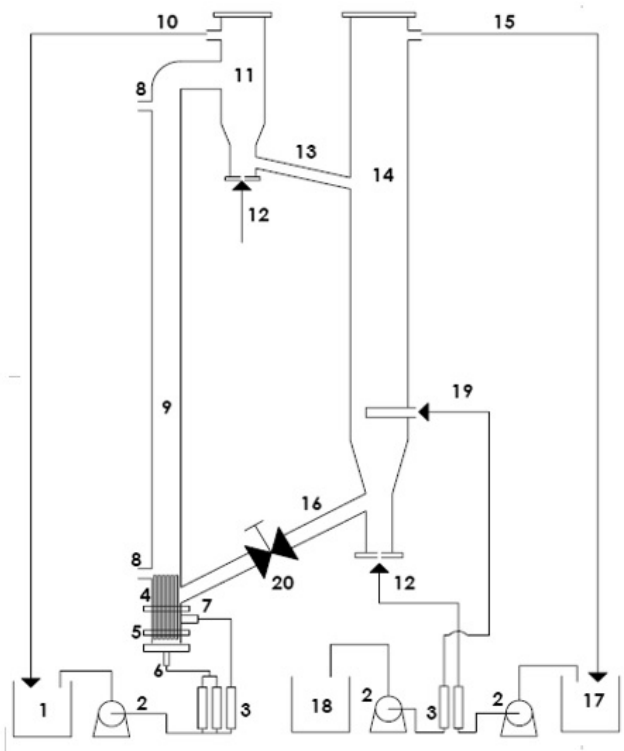

Figure 1. Schematic diagram of the experimental setup used. (1) Feed Tank; (2) Pump; (3) Rotameter; (4) Primary Distributor; (5) Secondary Distributor; (6) Primary Feed Line; (7) Secondary Feed Line; (8) Pressure Tapings; (9) Riser; (10) Liquid-Solid Separator Outlet; (11) Liquid-Solid Separator; (12) Wash Water; (13) Top Dynamic Seal; (14) Downcomer; (15) Downcomer Outlet; (16) Bottom Dynamic Seal; (17) Wash Water Storage Tank; (18) Desorption Liquid Storage Tank; (19) Desorption Liquid Inlet; (20) Check Valve.

2.4.1. Adsorption Cycle

The column was washed with water before operating it at the required conditions. The adsorbent was fed into the column to fill 35% of the riser height. The feed tank was filled with 1000 ppm stock solution. Primary liquid was pumped into the LSCFB through calibrated flow meters at a rate of 1100 L/h. The secondary feed was pumped at 750 L/h. The combined velocity offered by the primary and secondary feed streams was higher, which enabled the particles to move up at a velocity higher than the terminal velocity and less than the critical velocity. At this flow condition, the adsorbents got entrained by the liquid flowing vertically up in the riser and was passed to the liquid-solid separator. A solid hold up developed in the liquid-solid separator allowing for more interactions between the adsorbent and the adsorbate. Subsequently, the bulk and solid phases entered into the downcomer section of the LSCFB. The downcomer facilitated further adsorption due to a higher residence time offered by its larger diameter. The bulk phase flowed back into the riser through the bottom dynamic seal that was regulated using a valve. The column was run for 50 min and 10 mL solutions were withdrawn from the feed tank after proper mixing at 5 min intervals up to 50 min. The solution samples were then analyzed using a UV-V is spectrophotometer for its absorbance. The feed was then drained from the column to begin the desorption cycle after the water wash.

2.4.2. Desorption Cycle

The column was water-washed again, before its next run. The desorption liquid feed tank was supplied with a 5% (*v*/*v*) ethanol-water solution. It was pumped into the downcomer at a liquid flow rate of 1200 L/h. The direction of flow was reversed and the contents flowed backward into the liquid-solid separator and into the riser. The column ran for 50 min and samples of 10 mL volume were withdrawn from the desorption feed tank after proper mixing at 5 min intervals. The obtained samples were examined using a UV-Vis spectrophotometer for its absorbance. The bulk phase was then removed from the column and the adsorbent was analyzed through SEM.

3. Results

3.1. Batch Study

3.1.1. Effect of Adsorbent Dosage

The performance of the activated-carbon glass beads as a phenol removal adsorbent was mainly assessed by two factors: (i) the phenol-removal efficiency and (ii) the adsorption capacity [19]. The effect of the adsorbent dosage on these performance factors of the adsorbent was analyzed through batch adsorption experiments. For all the adsorbent dosages considered, the Langmuir isotherm produced a better correlation coefficient (R^2 = 0.9431) as compared to the Freundlich isotherm (R^2 = 0.9073) and, hence, the q_m value was analyzed for the factor of adsorption capacity for the various adsorbent dosages.

The phenol-removal efficiency is linked to the availability of active sites for the phenol molecules to get adsorbed [20,21]. On the other hand, the adsorption capacity is associated with the saturation of the binding spots on the adsorbent for the adsorbate to get adsorbed [22]. On analyzing the graph as shown in Figure 2a, it was seen that 1 g of the adsorbent produced the same percentage of adsorption for the various contact times and hence it was considered to be an ineffective dosage. For the case of 1.5 g of adsorbent dosage, better results were produced than 1 g in terms of the phenol-removal efficiency for a relatively lower value of adsorption capacity, but reached saturation at 65% itself, which was undesirable. Additionally, 2 and 2.5 g of adsorbent dosage produced approximately the same but much better results compared to 1 g and 1.5 g, resulting in a 78% and 80% phenol-removal efficiency, respectively, thus making it redundant to continue our experimentation of the batch studies with higher adsorbent loadings. Hence, it was concluded that 2.5 g of activated carbon yielded a desirable and effective phenol removal of 80% from the feed solution. This showed that despite having the least adsorption capacity among the various dosage runs, the adsorbent still possessed

considerable amount of vacant active sites for phenol adsorption and this would lead to better results (>80% phenol-removal efficiency) in the continuous LSCFB system.

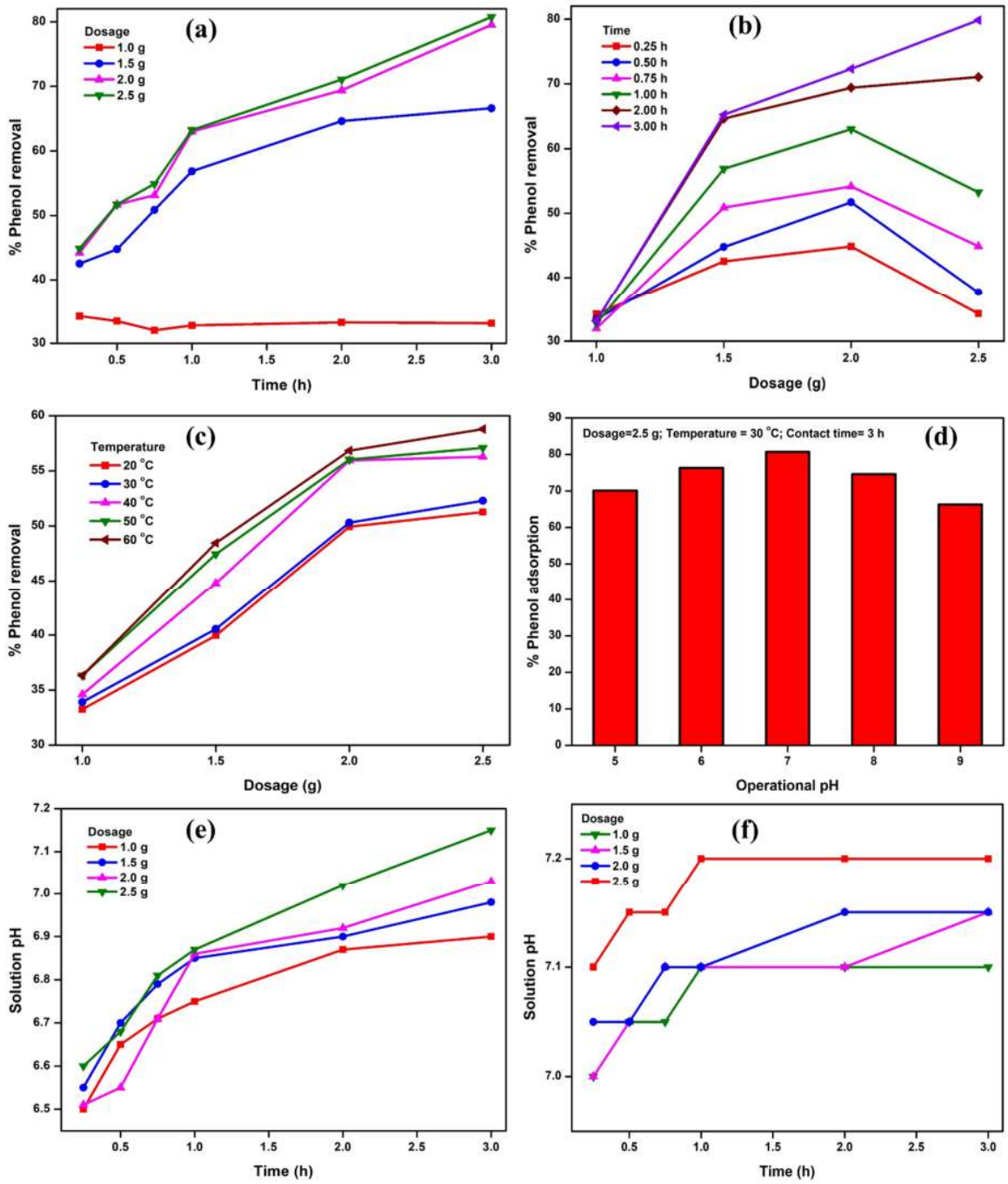

Figure 2. Effect of (**a**) adsorbent dosage; (**b**) contact time; (**c**) temperature and (**d**) operational pH on % phenol removal. Solution pH studies for (**e**) the adsorption system (phenol-activated carbon) and (**f**) control system (distilled-water-activated carbon).

3.1.2. Effect of Contact Time

As shown in Figure 2b, with an increase in adsorbent loading, it took more time for the bulk of the activated-carbon-coated glass beads to come into contact with the phenol solution, thus promoting increased interactions between the adsorbate and adsorbent [23]. This can be explained from the results portrayed in the figure. For instance, 1 g being the lowest adsorbent loading, it took less time

for the bulk of the beads to come in contact with the phenolic solution and hence all contact times had approximately the same phenol-removal efficiency. Moreover, as the adsorbent loading increased, it was evident that the larger adsorbent loadings took a longer time to reach an effective phenol-removal efficiency. For example, a 2.5 g loading showed variation in the adsorption percentage from a minimum of 35% adsorption in the first 0.25 h to a maximum of 80% adsorption within the next 3 h. Additionally, another reason for the trend observed is linked to the excessive contact time to which the system was subjected to. As the contact time increased, the system reached a point wherein the binding sites on the adsorbent become saturated and no more adsorption was practically possible. On closely observing the 3 h timeline for the four adsorbent loadings, it was evident that the phenol-removal efficiency increased with incremental levels of adsorbent dosage. This shows that the beads with an adsorbent loading of 2.5 g would produce the best results of >80% phenol removal for an optimal time of 3 h. With respect to the LSCFB, running the column at an appropriate adsorbent loading for a lesser amount of time was the viable option to maintain the surface morphology of the activated-carbon-coated glass beads.

3.1.3. Effect of Temperature

Generally, the behavior of the phenol–water system for temperature variations is very similar to that of a normal aqueous system till the attainment of the critical temperature of the binary system [4]. In this case, with the initial phenol solution taken being very dilute (1000 ppm) and the critical temperature of the system being ~70 °C, it was safe to increase the temperature of the solution till 60 °C. It is a very well-known and understood fact that on increasing the temperature of the solution, the kinetic energy of the molecules increases, which in turn increases the interaction between the adsorbate and the adsorbent, leading to more binding of the phenol on the adsorbent and hence an increased percentage adsorption [19].

From the graph as depicted in Figure 2c, it was observable that, at higher temperatures, all the four adsorbent dosages followed the same trend as explained earlier and displayed better percentages of adsorption for increased temperatures. For 1 g of adsorbent dosage, it was observed that the phenol-removal percentage was very less, at 35% for all the temperatures. However, higher dosage values of 1.5, 2 and 2.5 g showed better percentages of adsorption with an increase in operational temperature. For the optimal loading of 2.5 g, the phenol-removal efficiency was increased from 51% at 20 °C to 58.5% at 60 °C. Additionally, no significant increase in the phenol adsorption percentage for the temperature increment from 20 to 60 °C was observed. This in turn indicated that a relatively low operational temperature is more preferable for the phenol removal studies in the LSCFB. For the continuous column study, an operational temperature of 30 °C was selected as this was very close to the average room temperature of the current research work environment.

3.1.4. pH Variation Studies

The operational pH of the adsorption system is an important parameter that impacts the phenol-removal efficiency from the feed wastewater. In this study, the pH dependency examinations were performed by varying the operational pH in the range of 5 (acidic condition) to 9 (basic condition). Other parameters, such as dosage, contact time and temperature for the experimental tests, were fixed at conditions of 2.5 g, 3 h and 30 °C, respectively. Results for the influence of pH on the % phenol removal is presented in Figure 2d. A maximum phenol-removal efficiency of 80% was observed at a neutral pH of 7. Both the acidic (pH < 7) and basic (pH > 7) operational pH values resulted in a lower phenol-removal performance. Furthermore, the % phenol removal was comparatively lower in the basic environment than in the acidic environment. This was mainly due to the interference of the basic OH ions that hindered the diffusional effects of the phenol molecules into the pores of the activated carbon [4].

Further, in the batch experiments, continuous removal of phenol by the activated-carbon glass beads altered the pH value of the bulk solution [24]. The change in the pH value of the bulk phase would alter the instantaneous adsorption phenomenon for a given adsorbent dosage value. Figure 2e

presents the variation of the solution pH for the four adsorbent dosages at different contact times. It was seen that for lower adsorbent dosages and for smaller intervals of time, the pH values were closer to 6.5. While, on the contrary, for higher adsorbent loadings kept for a longer time, say until 3 h, the pH values reached a neutral value of 7. In order to ensure the attainment of a neutral pH by the bulk phase for higher adsorbent dosage and contact time, control runs were performed using distilled-water-activated carbon beads to understand the variation of solution pH. Results for the control run are presented in Figure 2f, which show a slight increment in the solution pH with increased time and adsorbent dosage. The trivial increase in the solution pH could be ascribed to the basic functional groups present on the surface of the activated carbon. This confirmed that the attainment of a neutral pH for the investigated phenol-activated carbon glass beads system was predominately due to the adsorptive removal of phenol from the bulk phase by the activated-carbon glass beads.

In general, the pH of a dilute phenolic solution having a concentration of 1000 ppm (0.01 M or 1 N) or less possessed a weak acidic character with its pH ranging from 6 to 7. The pH of the initial solution of 1000 ppm concentration before subjecting to adsorption study was 6.2, as calculated using a pH meter. The ability of phenol to exhibit a weak acidic character despite the presence of an −OH group is attributed to the stability of the benzene ring. Phenol loses an H^+ ion-producing phenoxide ion that stabilizes itself by delocalizing the negative ion with the pie bonds throughout the ring [25,26].

3.1.5. Desorption Study

As shown in Figure 3, the regeneration of the phenol-adsorbed activated-carbon glass beads using a 5% (*v*/*v*) ethanol solution was performed by assessing the desorption potential of the phenol from the activated-carbon-coated glass beads in presence of an ethanol medium [27]. From the obtained results, it was clear that using a 5% (*v*/*v*) ethanol solution resulted in a 56% phenol desorption efficiency for the activated-carbon-coated glass beads for a regeneration period of 2 h. Hence, the viable option while working with the downcomer of the LSCFB would be increasing the concentration of the ethanol solution that can bring about a satisfactory desorption or removal of phenol from the beads within a lesser amount of time.

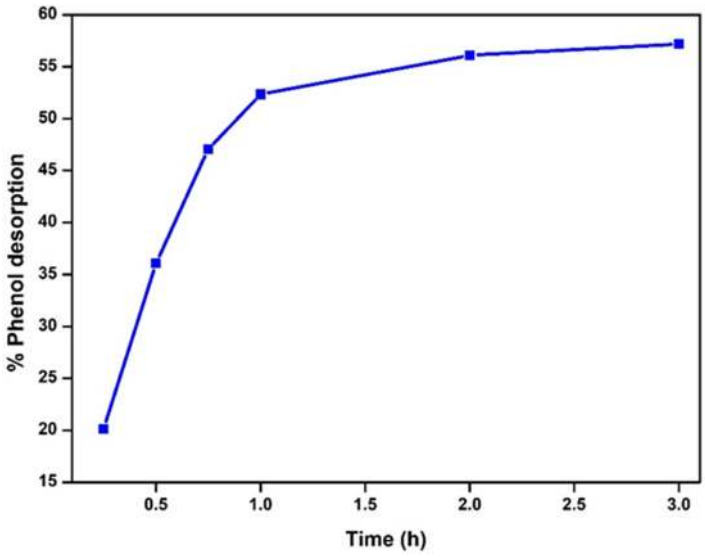

Figure 3. The % desorption of phenol over time with the use of 5% (*v*/*v*) ethanol.

3.1.6. Adsorption Isotherms

The Langmuir and Freundlich isotherm models were examined to predict the interactive nature between the phenol and activated-carbon glass beads. The Langmuir isotherm postulates the theory of energetically equivalent active sites of the sorbent. Accordingly, the adsorption would result in a single layer formation of adsorbate on the adsorbent. The isotherm advocates a characteristic theoretical

maximum of adsorption capacity (q_{max}). According to Langmuir, the relation between C_e and q_e in a linearized form is shown in Equation (3) [28]:

$$\frac{C_e}{q_e} = \frac{1}{q_m K_L} + \frac{C_e}{q_m} \tag{3}$$

where q_m (mg/g) and K_L (L/mg) are the monolayer maximum adsorption capacity and the adsorption constant for Langmuir isotherm, respectively. The separation factor (R_L) explicates the favor of adsorption if $0 < R_L < 1$ and is given by Equation (4) [29]:

$$R_L = \frac{1}{1 + K_L C_i} \tag{4}$$

The Freundlich isotherm supports the heterogeneous and rough surface nature of the solid phase. The isotherm highlights the existence of interactions between the surface-bonded and free molecules of the liquid phase, which results in multilayer formation of the sorbate molecules. The Freundlich isotherm relates C_e and q_e linearly, as presented in Equation (5) [30]:

$$\ln(q_e) = \ln\left(K_f\right) + \frac{1}{n}\ln(C_e) \tag{5}$$

where K_f ($mg^{1-1/n}\ L^{1/n}\ g^{-1}$) and n are the adsorption constant for the Freundlich isotherm and the adsorption intensity, respectively.

Results of the equilibrium modeling with experimental data are shown in Figure 4. The values of the Langmuir (K_L) and Freundlich (K_f) constants were evaluated as 0.0062 L/mg and 1.9051 $mg^{1-1/n}\ L^{1/n}/g$, respectively. Various other isotherm parameters are tabulated in Table 1. The higher R^2 value of the Langmuir isotherm showed that the phenol adsorption on the activated carbon glass beads was homogenous with monolayer formation. The separation factor (R_L) was calculated from the Langmuir constant (K_L) and the initial concentration of the solution (C_0). The ideal range for R_L is theoretically estimated to be between 0 and 1. When the R_L value is in the range of 0 to 1, the resultant adsorption process is said to be a favorable process. On the contrary, any value of $R_L > 1$ indicates that the adsorption process is reversible. The separation factor for the reported adsorption batch study using a 2.5 g adsorbent dosage was estimated to be 0.1398, which substantiated the fact that the adsorption of phenol on activated-carbon-coated glass beads was physisorption [31].

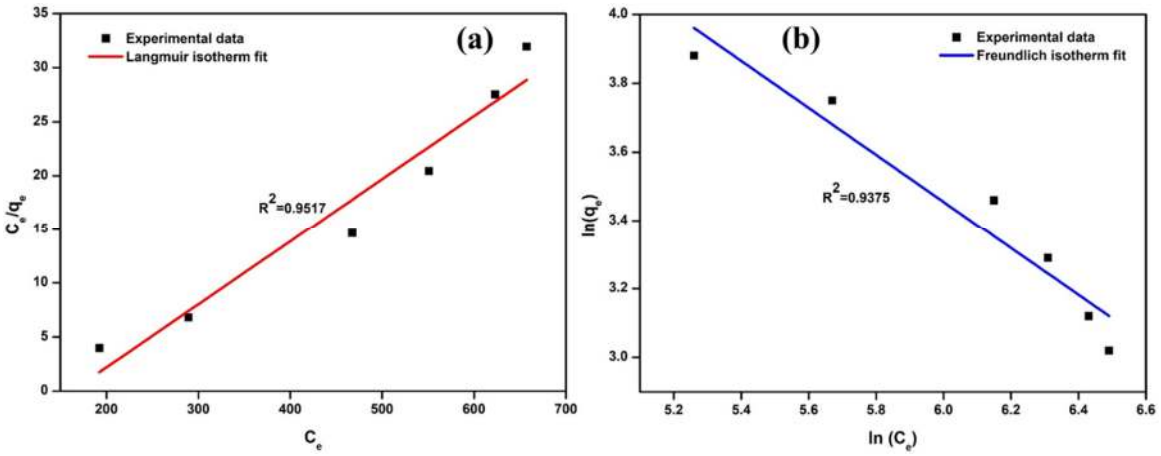

Figure 4. Adsorption isotherms: (**a**) The Langmuir isotherm for an adsorbent dosage of 2.5 g; and (**b**) the Freundlich isotherm for an adsorbent dosage of 2.5 g.

Table 1. Equilibrium isotherm parameters.

Isotherm	Parameters	Values
Langmuir	R^2	0.9571
	q_m (mg/g)	17.12
	K_L (L/mg)	0.0062
	R_L	0.1398
Freundlich	R^2	0.9375
	n	1.4643
	K_f ($mg^{1-1/n}$ $L^{1/n}$/g)	1.9051

3.2. Column Study

3.2.1. Operational Parameters

The LSCFB was designed and fabricated to run for two cycles, namely, the adsorption and desorption cycle, operated for a total duration of 50 min per cycle and maintaining a primary flow rate of 1100 L/h and a secondary flow rate of 750 L/h. The operating feed volume was maintained at 35% of the total volume of the riser, whose dimensions were 1.5 m in height and 0.04 m in diameter. All the experiments were carried out at a room temperature of 30 °C. The solid holdup was estimated by the pressure gradient in the riser. On eliminating any kind of effects due to wall friction, the average solid holdup (ε_s) was determined using Equations (6) and (7).

$$-\frac{\Delta P}{\Delta L} = (\varepsilon_s \rho_s + \varepsilon_1 \rho_1) g \tag{6}$$

$$\varepsilon_s + \varepsilon_1 = 1 \tag{7}$$

where $\frac{\Delta P}{\Delta L}$, ε_s ε_1, ρ_s, ρ_1 and g are the pressure drop gradient (N/m^3), solid holdup, liquid holdup, density of the solid (kg/m^3), density of the liquid (kg/m^3) and acceleration due to gravity (m/s^2), respectively.

The value of the terminal velocity (u_{tr}) of the particle is theorized to be estimated from Equation (8). This value tends to be greater than the minimum fluidization velocity of the particle for the liquid.

$$u_{tr} = \left[\frac{4(\rho_s - \rho_l)^2 g^2}{225 \rho_l \mu}\right]^{\frac{1}{3}} d_p \tag{8}$$

where d_p and μ are the solid diameter (m) and the liquid viscosity (kg/m s).

The cumulative flow rate of the primary and the secondary inlet pipes provided the total net liquid flow rate. The critical velocity being greater than the terminal velocity of the particle is given by Equation (9) [32,33]:

$$u_{cr} = 1.2 * u_{tr} \tag{9}$$

The column was operated above the terminal velocity and below the critical transition velocity. The operational conditions of the LSCFB are enlisted in Table 2 [18].

3.2.2. Adsorption Cycle

From the experimental data achieved, it was evident that the LSCFB facilitated a better adsorbate-adsorbent interaction. This was corroborated from the results presented in Figure 5a that showed that the phenol-removal efficiency in the LSCFB was 98%, which was 18% more than the phenol-removal efficiency achieved by 2.5 g of adsorbent dosage in the batch study; also, this enhancement in the phenol-removal efficiency was achieved in a very short operation time of 25 min, as compared with the 3 h contact time of the batch mode.

Table 2. Operational parameters for the liquid-solid circulating fluidized bed (LSCFB) column.

Primary Liquid Flow Rate (L/h)	1100
Secondary Liquid Flow Rate (L/h)	750
Desorption Liquid Flow Rate (L/h)	1200
Archimedes Number	56,108
Terminal Velocity of Adsorbent (m/s)	0.2783
Minimum Fluidization Velocity (m/s)	0.0180
Critical Velocity (m/s)	0.3340
Pressure Drop (N/m^2)	701.19
Solid Holdup	0.5193
Liquid Holdup	0.4087

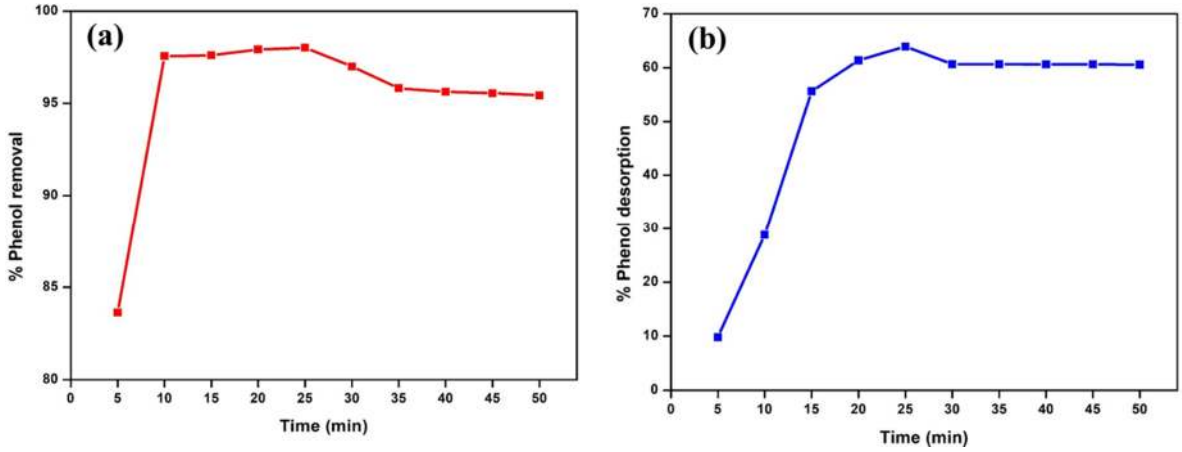

Figure 5. (**a**) The % phenol removal vs. time in an LSCFB; and (**b**) % phenol desorption vs. time in an LSCFB.

3.2.3. Desorption Cycle

An adsorbent dosage of 2.5 g in the batch study produced a maximum of 56% desorption. Under the same conditions, the continuous column study using the LSCFB resulted in a 64% desorption in a lesser time of 20 min, as shown in Figure 5b. Hence, it was primarily evident that a continuous flow system enriched the desorption level of the adsorbent compared to the batch mode. Additionally, it was also interpreted that on increasing the ethanol concentration, better desorption rates can be achieved in a lesser period.

3.2.4. Column Adsorption Models

On plotting the breakthrough curve for the column [34], a skewed S-shaped curve was obtained, as shown in Figure 6a, which signified the different packing densities in the bed provided by the solid and liquid voidage, thus maintaining the heterogeneity of the bed.

Further modeling was carried out using the Yoon-Nelson, Adam-Bohart and modified-dose response models. The results for the analysis of various column models are presented in Figure 6b–d. The Yoon-Nelson model for column adsorption is described by Equations (10,11) [35]:

$$\ln\left[\frac{C_t}{C_0 - C_t}\right] = k_{YN}t - k_{YN}\tau \tag{10}$$

$$q_{YN} = \frac{C_0\, Q\tau}{1000\, w} \tag{11}$$

where, k_{YN}, τ, Q, w and q_{YN} are the rate constant (1/min), time required for 50% adsorbate breakthrough (min), flow rate (L/min), weight of the adsorbent (g) and Yoon-Nelson adsorptive capacity of the bed (mg/g).

The Adam-Bohart model is based on the theory that the concentration of the feed solution is weak with the speed of adsorption limited by external mass transfer [36]. The model is explained by Equation (12), which relates the value of C_0/C_t with time (t) in an open system. It has been formulated as follows:

$$\ln\left[\frac{C_0}{C_t} - 1\right] = \left(\frac{k_{AB}N_0Z}{u}\right) - k_{AB}C_0t \quad (12)$$

where, k_{AB}, Z, N_0 and u are the kinetic constant (L/g/min), bed depth in the column (m), Adam-Bohart adsorptive capacity of the bed (mg/g) and outlet velocity of the bed (m/min).

The modified dose-response (MDR) model is a topical fit variant for the column adsorption studies. It is a non-linear logistic fit mostly used to describe the column adsorption behavior of heavy metals. The model is described by the non-linear correlation as specified in Equations (13) and (14) [37].

$$\frac{C_t}{C_0} = 1 - \frac{1}{\left(\frac{ut}{b} + 1\right)^a} \quad (13)$$

$$q_{MDR} = \frac{C_0\, b}{w_a} \quad (14)$$

where a and b (mL) are the characteristic factors of the MDR model.

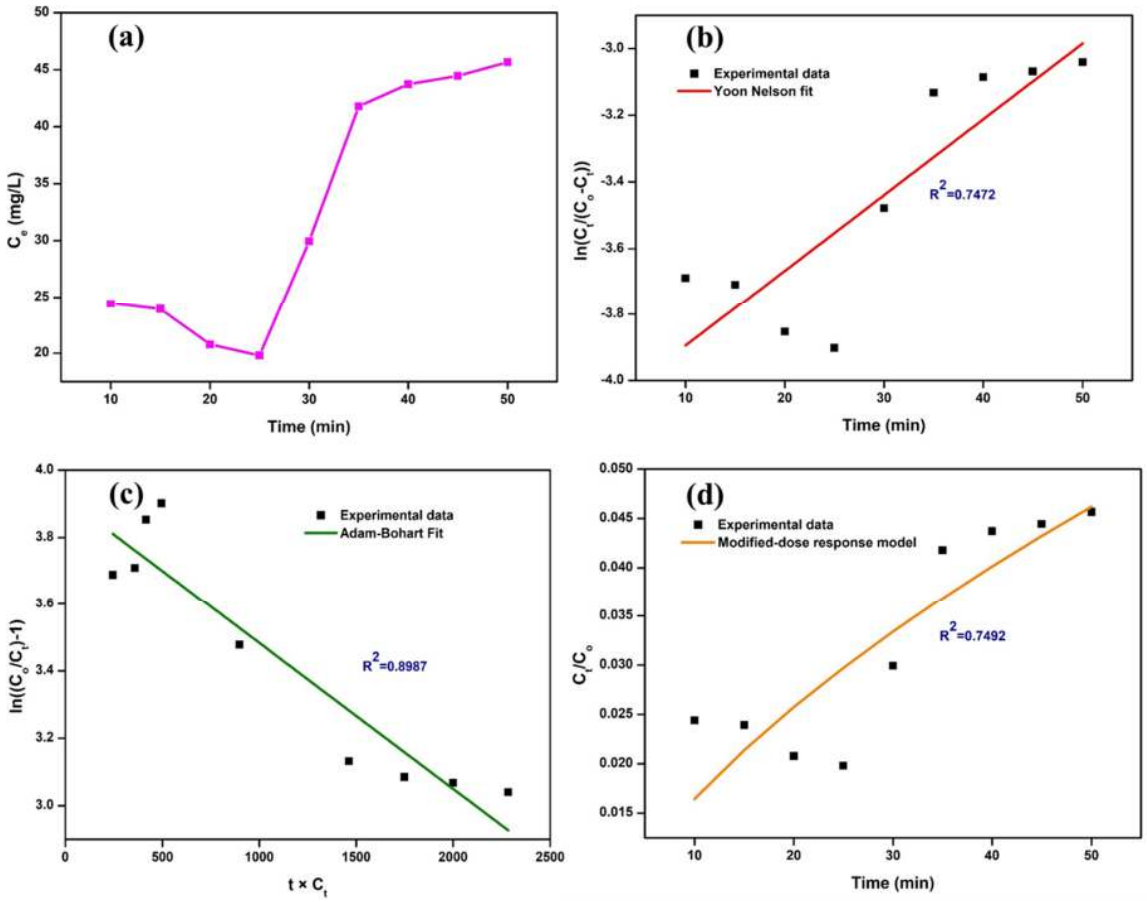

Figure 6. (**a**) Phenol-activated carbon breakthrough curve analysis; (**b**) Yoon-Nelson fit model; (**c**) Adam–Bohart fit model; and (**d**) modified-dose response model.

Table 3 presents the characteristic column adsorption capacity obtained for the experimental studies as well as using various theoretical models examined for the column adsorption. The higher correlation coefficient of R^2 = 0.8987 indicated that the column adsorption studies obeyed the Adam-Bohart model. The adsorbent capacity predicted by this model was also very close to that of the experimental values. This showed that the column adsorption of phenol onto the activated-carbon-coated glass beads involved a quasi-chemical interactions along with the absence of the internal diffusion effects of the bulk phase on the solid phase [36].

Table 3. Column study—Adsorption modeling.

Model	Characteristic Parameter	Parameter Value	R^2
Breakthrough curve	Bead Capacity (BC)	250 mg/g	-
Yoon-Nelson	Adsorbent Capacity (q_{0YN})	163 mg/g	0.7472
Adam-Bohart	Adsorbent Capacity (N_0)	279 mg/g	0.8987
Modified-dose response	Adsorbent Capacity (q_{MDR})	291 mg/g	0.8492

3.3. SEM Analysis

The morphology of the fresh, spent and regenerated activated-carbon glass beads was studied by the SEM technique. The micrographs obtained for the adsorbent beads are presented in Figure 7. As shown in Figure 7a, the activated carbon possessed a cellular and honeycomb-like structure, despite the process undergone in the preparation of the adsorbent using the glass beads, epoxy resin and activated carbon. The thin porous sheet-like structure of the adsorbent was homogenously distributed, which elevated the pore density of the activated carbon beads. These numerous pores hosted the necessary active sites for phenol adsorption [38].

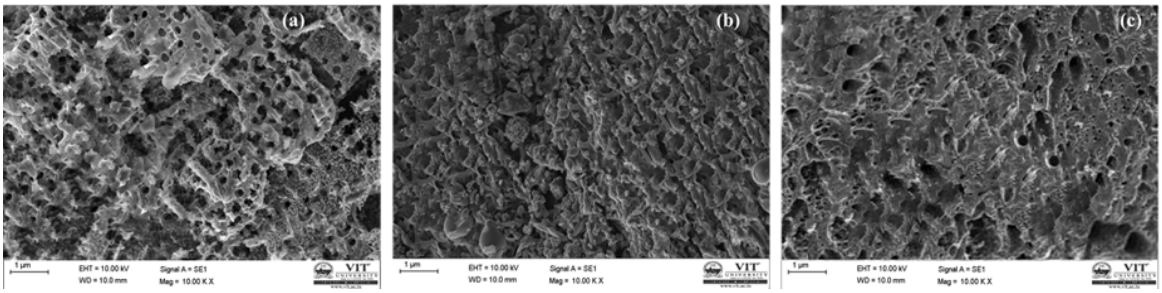

Figure 7. SEM micrographs of the activated-carbon-coated glass beads: (**a**) before adsorption; (**b**) after adsorption; and (**c**) after desorption.

The SEM image for the spent adsorbent (Figure 7b) showed the successful adsorption of the phenol molecules on the activated-carbon-coated glass beads. The densified nature of the adsorbent with complete coverage of the porous honeycomb structure confirmed the phenol binding to the adsorbent surface. The micrograph also showed a uniform coverage of the active sites by the phenol molecules, which indicated the energetically homogenous nature of the activated-carbon glass beads [39].

Figure 7c depicts the regenerated surface of the activated-carbon-coated glass beads. The quasi-porous nature of the regenerated adsorbent clearly showed that the ethanol medium efficiently desorbed the phenol molecules from the pores of the adsorbent, allowing the reuse of the adsorbent in the LSCFB.

3.4. FTIR Analysis

The surface chemistry of the activated-carbon glass beads at different stages of the experiment was analyzed using the FTIR technique. Figure 8 and Table 4 contain the results for the pristine adsorbent. The characteristic stretch observed at 3626.17 cm^{-1} was due to the –OH band of the adsorbed water whereas the peaks at 3095.75 cm^{-1} and 3066.82 cm^{-1} were due to the –OH vibrations of the carboxylic

acids group present in the activated carbon. The spectra showed the presence of peaks in the fingerprint region, which corresponded to the presence of SiO_2 and C–C bonds, thus confirming the presence of glass beads and activated carbon, respectively. The epoxy resin ($C_{21}H_{25}ClO$) showed a strong C–Cl presence in the infrared region between 800 and 600 cm^{-1}. The large number of teeth-like structures was attributed to the occurrence of vibrations of the C–C bonds when subjected to infra-red radiation. The absence of other peaks throughout the entire wavelength region confirmed that the adsorbent contained only the aforementioned compounds [40].

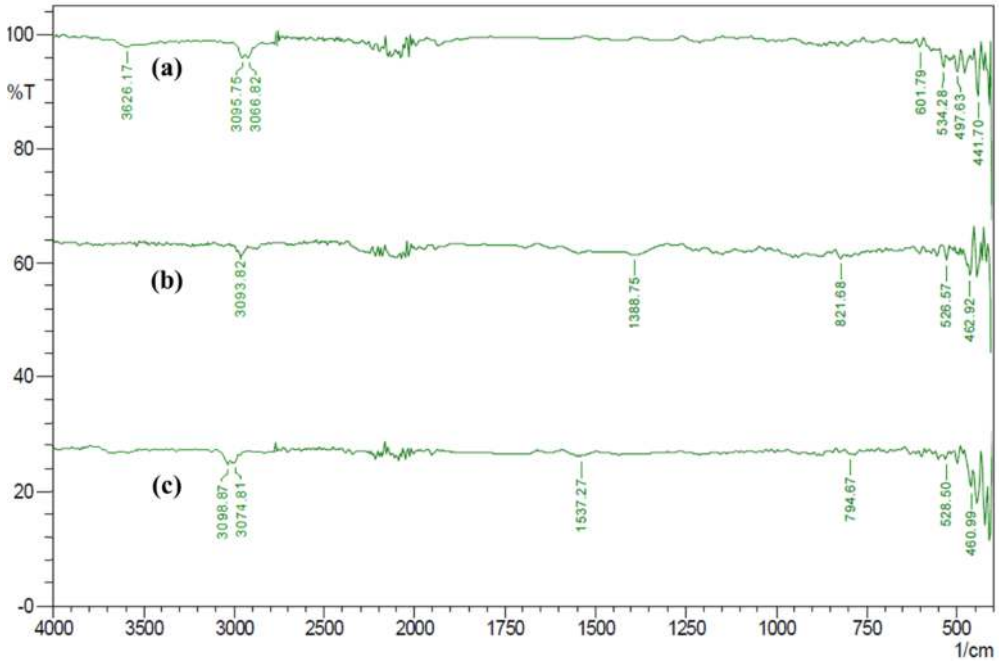

Figure 8. FTIR analysis of the adsorbent: (**a**) before adsorption; (**b**) after adsorption; and (**c**) after desorption.

Table 4. FTIR functional group analysis for the activated-carbon beads.

Wavelength Region (cm^{-1})	Functional Group	Compound
Fresh activated-carbon beads		
600–400	-	SiO_2 (Glass Beads)
Teeth-like structures between 1500 and 600	-	C–C (Activated Carbon)
800–600	C–Cl	Epoxy Resin
Spent activated-carbon beads		
1410–1310	–OH	Phenol
Teeth-like structures between 2500 and 2000	Aromatic (Benzene)	C = C (Strong)
900–700	Aromatic (Benzene)	C = C (sp^2 C–C)
Regenerated activated-carbon beads		
1600–1400	Aromatic (Benzene)	C = C (Weak)
Teeth-like structures between 2500 and 2000	Aromatic (Benzene)	C = C
800–590	–OH	Ethanol (Weak)

FTIR spectra for the phenol-adsorbed activated-carbon glass beads are presented in Figure 8 and Table 4. The results indicated the presence of phenol at a stretch between 1410 and 1310 cm^{-1} and at an appropriate value of 1388.75 cm^{-1}. Secondly, the prevalence of teeth-like structures between 2500 and 2000 cm^{-1} showed strong C = C functionality due to the presence of an aromatic ring. Moreover, the existence of a benzene ring in phenol adsorbed by the adsorbent can be confirmed by the peak at 821.68 cm^{-1}. Given the fact that the solutions taken were dilute, peaks were not obtained between 3200 and 3100 cm^{-1}, which would have indicated an alcohol-water solution in the system. The red shift in the –OH band from 3095.75 cm^{-1} (pertaining to fresh adsorbent) to 3093.82 cm^{-1} indicated the

interactions of the carboxylic groups present in the adsorbent for phenol adsorption. Additionally, the peaks obtained in the fingerprint region adhere to those previously obtained, thus proving that no other compounds were formed during adsorption [41].

The results for surface functionality of the ethanol-washed adsorbent beads are presented in Figure 8 and Table 4. The presence of a peak at 794.67 cm^{-1} indicated the weak presence of an alcohol group, which was possibly ethanol. Secondly, the broad stretch between 1600 and 1400^{-1} with a peak at 1537.27 cm^{-1} showed a weak aromatic character, which indicated the reduced aromatic tendencies as compared to Figure 8b. This confirmed the successful desorption of phenol in the regenerated adsorbent beads; also, the restoration of the characteristic bands at positions 3098.87 cm^{-1} and 3074.81 cm^{-1} confirmed the successful regeneration of the adsorbent beads. The presence of no other peaks highlighted that no other side compounds were formed that led to any changes in the system and both adsorption and desorption occurred successfully. Additionally, the fingerprint region remained the same as before.

4. Conclusions

In this study, activated-carbon-coated glass bead adsorbents were developed and applied for phenol removal from synthetic wastewater. Batch adsorption studies indicated a maximum phenol removal of 80% for the optimal operational conditions of an adsorbent dosage 2.5 g, contact time 3 h and temperature 30 °C. Reusability studies of the adsorbent beads using a 5% (*v*/*v*) ethanol solution showed a good regeneration percentage of 56%, which were associated with the activated-carbon beads for phenol removal studies. To further enhance the performance of the phenol-removal process using the as-developed activated-carbon beads, a column study was performed in an LSCFB. A very high phenol-removal efficiency of 98% was achieved in the LSCFB with an enhanced regeneration efficiency of 64% for the adsorbent beads, within a shorter duration of 20 min (as compared to batch adsorption results). The results analyzed from the batch and column study indicated that the Langmuir and Adam-Bohart models provided the best fit, respectively. This elucidated the monolayer deposition of the phenol on the adsorbent beads through a quasi-chemical reaction phenomenon. Furthermore, the morphological analysis of the adsorbent beads at various stages of adsorption and regeneration studies exhibited their intact structural stability. Furthermore, surface chemistry studies of the adsorbent using the FTIR technique showed that the chemical functionality of the adsorbent was well maintained, and that successful phenol adsorption/desorption occurred on the surface of the activated-carbon glass beads. The results highlighted that the continuous mode of phenol removal and adsorbent regeneration using the LSCFB was more advantageous and significant than the batch mode. Thus, phenol removal using activated-carbon-coated glass beads in an LSCFB is reported as a novel approach for effective treatment of phenol-polluted wastewater streams. The promising results of the study indicate the possible industrial potential of the presented technique, especially towards toxic phenol contaminant elimination from aqueous solutions.

Author Contributions: Conceptualization, N.G. and R.K.; methodology, N.S., S.B. and S.S.; software, N.G. and R.K.; data curation, N.S., S.B. and S.S.; data validation, N.G., R.K. and P.L.S.; writing—original draft, N.S., S.B., S.S. and R.K.; writing—review and editing, N.G., M.T., F.A. and H.A.; project administration, N.G., M.T. and R.K.; funding acquisition, N.G. and H.A. All authors have read and agreed to the published version of the manuscript.

Funding: This research received no external funding.

Acknowledgments: The authors are grateful to the Vellore Institute of Technology, Vellore, for providing SEED money and an efficient infrastructure facility to carry out the present study, as well as for providing a scanning electron microscopy analysis facility aided by DST-FIST-SBST-VIT (SEM EVO 18, CARL ZEISS).

Conflicts of Interest: The authors declare no conflict of interest.

References

1. Bharath, G.; Hai, A.; Rambabu, K.; Banat, F.; Ashraf, M.T.; Schmidt, J.E. Systematic production and characterization of pyrolysis oil from date tree wastes for bio-fuel applications. *Biomass Bioenergy* **2020**, *135*, 105523. [CrossRef]
2. Pernyeszi, T.; Farkas, V.; Felinger, A.; Boros, B.; Dékány, I. Use of non-living lyophilized Phanerochaete chrysosporium cultivated in various media for phenol removal. *Environ. Sci. Pollut. Res.* **2018**, *25*, 8550–8562. [CrossRef] [PubMed]
3. Ali, A.; Bilal, M.; Khan, R.; Farooq, R.; Siddique, M. Ultrasound-assisted adsorption of phenol from aqueous solution by using spent black tea leaves. *Environ. Sci. Pollut. Res.* **2018**, *25*, 22920–22930. [CrossRef] [PubMed]
4. Nirmala, G.; Murugesan, T.; Rambabu, K.; Sathiyanarayanan, K.; Show, P.L. Adsorptive removal of phenol using banyan root activated carbon. *Chem. Eng. Commun.* **2019**, 1–12. [CrossRef]
5. Bharath, G.; Hai, A.; Rambabu, K.; Savariraj, D.; Ibrahim, Y.; Banat, F. The fabrication of activated carbon and metal-carbide 2D framework-based asymmetric electrodes for the capacitive deionization of Cr(vi) ions toward industrial wastewater remediation. *Environ. Sci. Water Res. Technol.* **2020**, *6*, 351–361. [CrossRef]
6. Evangeline, C.; Pragasam, V.; Rambabu, K.; Velu, S.; Monash, P.; Arthanareeswaran, G.; Banat, F. Iron oxide modified polyethersulfone/cellulose acetate blend membrane for enhanced defluoridation application. *Desalin. Water Treat.* **2019**, *156*, 177–188. [CrossRef]
7. Krishnamoorthy, R.; Govindan, B.; Banat, F.; Sagadevan, V.; Purushothaman, M.; Show, P.L. Date pits activated carbon for divalent lead ions removal. *J. Biosci. Bioeng.* **2019**, *128*, 88–97. [CrossRef]
8. Hai, A.; Bharath, G.; Babu, K.R.; Taher, H.; Naushad, M.; Banat, F. Date seeds biomass-derived activated carbon for efficient removal of NaCl from saline solution. *Process Saf. Environ. Prot.* **2019**, *129*, 103–111. [CrossRef]
9. Wang, J.; Shao, Y.; Yan, X.; Zhu, J. Review of (gas)-liquid-solid circulating fluidized beds as biochemical and environmental reactors. *Chem. Eng. J.* **2019**, *386*, 121951. [CrossRef]
10. Zhu, J.X.; Zheng, Y.; Karamanev, D.G.; Bassi, A.S. (Gas-)liquid-solid circulating fluidized beds and their potential applications to bioreactor engineering. *Can. J. Chem. Eng.* **2000**, *78*, 82–94. [CrossRef]
11. Zheng, Y.; Zhu, J.X.; Marwaha, N.S.; Bassi, A.S. Radial solids flow structure in a liquid-solids circulating fluidized bed. *Chem. Eng. J.* **2002**, *88*, 141–150. [CrossRef]
12. Lan, Q.; Bassi, A.S.; Zhu, J.X.; Margaritis, A. Continuous Protein Recovery with a Liquid-Solid Circulating Fluidized-Bed Ion Exchanger. *AIChE J.* **2002**, *48*, 252–261. [CrossRef]
13. Rao, V.V.B.; Rao, S.R.M. Adsorption studies on treatment of textile dyeing industrial effluent by flyash. *Chem. Eng. J.* **2006**, *116*, 77–84.
14. Foo, K.Y.; Hameed, B.H. Insights into the modeling of adsorption isotherm systems. *Chem. Eng. J.* **2010**, *156*, 2–10. [CrossRef]
15. Rambabu, K.; Velu, S. Improved performance of $CaCl_2$ incorporated polyethersulfone ultrafiltration membranes. *Period. Polytech. Chem. Eng.* **2016**, *60*, 181–191. [CrossRef]
16. Bharath, G.; Rambabu, K.; Hai, A.; Anwer, S.; Banat, F.; Ponpandian, N. Synthesis of one-dimensional magnetite hydroxyapatite nanorods on reduced graphene oxide sheets for selective separation and controlled delivery of hemoglobin. *Appl. Surf. Sci.* **2020**, *501*, 144215. [CrossRef]
17. Rambabu, K.; Bharath, G.; Banat, F.; Show, P.L. Biosorption performance of date palm empty fruit bunch wastes for toxic hexavalent chromium removal. *Environ. Res.* **2020**, *187*, 109694. [CrossRef] [PubMed]
18. Gnanasundaram, N.; Loganathan, M.; Perumal, K. Solid holdup in liquid solid circulating fluidized bed with viscous liquid medium. *Alexandria Eng. J.* **2014**, *53*, 959–968. [CrossRef]
19. Anjum, H.; Gnanasundaram, N.; Johari, K.; Murugesan, T. Decontamination of benzene from aqueous solution by green functionalization of activated carbon. In Proceedings of the IOP Conference Series: Materials Science and Engineering, Kuala Lumpur, Malaysia, 13–14 August 2018.
20. Oladipupo Kareem, M.; Edathil, A.A.; Rambabu, K.; Bharath, G.; Banat, F.; Nirmala, G.S.; Sathiyanarayanan, K. Extraction, characterization and optimization of high quality bio-oil derived from waste date seeds. *Chem. Eng. Commun.* **2019**, 1–11. [CrossRef]

21. Rambabu, K.; Hai, A.; Bharath, G.; Banat, F.; Show, P.L. Molybdenum disulfide decorated palm oil waste activated carbon as an efficient catalyst for hydrogen generation by sodium borohydride hydrolysis. *Int. J. Hydrogen Energy* **2019**, *44*, 14406–14415. [CrossRef]
22. Rambabu, K.; Show, P.-L.; Bharath, G.; Banat, F.; Naushad, M.; Chang, J.-S. Enhanced biohydrogen production from date seeds by Clostridium thermocellum ATCC 27405. *Int. J. Hydrogen Energy* **2019**, in press. [CrossRef]
23. Padmavathy, K.S.; Madhu, G.; Haseena, P.V. A study on Effects of pH, Adsorbent Dosage, Time, Initial Concentration and Adsorption Isotherm Study for the Removal of Hexavalent Chromium (Cr (VI)) from Wastewater by Magnetite Nanoparticles. *Procedia Technol.* **2016**, *24*, 585–594. [CrossRef]
24. Bharath, G.; Rambabu, K.; Banat, F.; Anwer, S.; Lee, S.; Binsaleh, N.; Latha, S.; Ponpandian, N. Mesoporous hydroxyapatite nanoplate arrays as pH-sensitive drug carrier for cancer therapy. *Mater. Res. Express* **2019**, *6*, 085409. [CrossRef]
25. Gaber, D.; Abu Haija, M.; Eskhan, A.; Banat, F. Graphene as an Efficient and Reusable Adsorbent Compared to Activated Carbons for the Removal of Phenol from Aqueous Solutions. *Water. Air. Soil Pollut.* **2017**, *228*, 320. [CrossRef]
26. Banat, F.; Al-Asheh, S.; Al-Makhadmeh, L. Utilization of raw and activated date pits for the removal of phenol from aqueous solutions. *Chem. Eng. Technol.* **2004**, *27*, 80–86. [CrossRef]
27. Delgado, J.A.; Uguina, M.A.; Sotelo, J.L.; Águeda, V.I.; Gómez, P.; Hernández, V. Modelling the desorption of ethanol from an externally heated saturated activated carbon column by purging with air. *Adsorpt. Sci. Technol.* **2010**, *28*, 689–704. [CrossRef]
28. Anjum, H.; Johari, K.; Gnanasundaram, N.; Appusamy, A.; Thanabalan, M. Investigation of green functionalization of multiwall carbon nanotubes and its application in adsorption of benzene, toluene & p-xylene from aqueous solution. *J. Clean. Prod.* **2019**, *221*, 323–338.
29. Anjum, H.; Johari, K.; Gnanasundaram, N.; Appusamy, A.; Thanabalan, M. Impact of surface modification on adsorptive removal of BTX onto activated carbon. *J. Mol. Liq.* **2019**, *280*, 238–251. [CrossRef]
30. Gnanasundaram, N.; Loganathan, M.; Singh, A. Optimization and Performance parameters for adsorption of Cr6+ by microwave assisted carbon from Sterculia foetida shells. In Proceedings of the IOP Conference Series: Materials Science and Engineering, Miri, Sarawak, Malaysia, 1–3 December 2016.
31. Sarma, G.K.; Sen Gupta, S.; Bhattacharyya, K.G. Nanomaterials as versatile adsorbents for heavy metal ions in water: A review. *Environ. Sci. Pollut. Res.* **2019**, *26*, 6245–6278. [CrossRef]
32. Gnanasundaram, N.; Venugopal, A.; Ullas, G.; Katragadda, Y. Effect of Liquid Viscosity and Solid Inventory on Hydrodynamics in a Liquid-solid Circulating Fluidized Bed. *J. Appl. Fluid Mech.* **2017**, *10*, 267–274.
33. Trivedi, U.; Bassi, A.; Zhu, J.X. (Jesse) Continuous enzymatic polymerization of phenol in a liquid-solid circulating fluidized bed. *Powder Technol.* **2006**, *169*, 61–70. [CrossRef]
34. Edathil, A.A.; Pal, P.; Kannan, P.; Banat, F. Total organic acid adsorption using alginate/clay hybrid composite for industrial lean amine reclamation using fixed-bed: Parametric study coupled with foaming. *Int. J. Greenh. Gas Control* **2020**, *94*, 102907. [CrossRef]
35. Patel, H. Fixed-bed column adsorption study: A comprehensive review. *Appl. Water Sci.* **2019**, *9*, 45. [CrossRef]
36. Shi, S.L.; Lv, J.P.; Liu, Q.; Nan, F.R.; Jiao, X.Y.; Feng, J.; Xie, S.L. Application of Phragmites australis to remove phenol from aqueous solutions by chemical activation in batch and fixed-bed columns. *Environ. Sci. Pollut. Res.* **2018**, *25*, 23917–23928. [CrossRef] [PubMed]
37. Song, J.; Zou, W.; Bian, Y.; Su, F.; Han, R. Adsorption characteristics of methylene blue by peanut husk in batch and column modes. *Desalination* **2011**, *265*, 119–125. [CrossRef]
38. Sriram, A.; Swaminathan, G. Utilization of dye-loaded activated carbon as a potential alternative fuel source: A feasibility study through calorific and thermo-gravimetric analysis. *Environ. Sci. Pollut. Res.* **2018**, *25*, 33140–33152. [CrossRef]
39. Omidi Khaniabadi, Y.; Jafari, A.; Nourmoradi, H.; Taheri, F.; Saeedi, S. Adsorption of 4-chlorophenol from aqueous solution using activated carbon synthesized from aloe vera green wastes. *J. Adv. Environ. Heal. Res.* **2015**, *3*, 120–129.

40. Pal, P.; Edathil, A.A.; Chaurasia, L.; Rambabu, K.; Banat, F. Removal of sulfide from aqueous solutions using novel alginate–iron oxide magnetic hydrogel composites. *Polym. Bull.* **2018**, *75*, 5455–5475. [CrossRef]
41. Rambabu, K.; Srivatsan, N.; Gurumoorthy, A.V.P. Polyethersulfone-barium chloride blend ultrafiltration membranes for dye removal studies. In Proceedings of the IOP Conference Series: Materials Science and Engineering, Vellore, Tamil Nadu, India, 2–3 May 2017; Volume 263.